EMRP ENV02 PartEmission

WP1
Task 1.1
Deliverable 1.1.2

Temperature resistant aerosol standards at 30 nm, 50 nm and 100 nm for number concentration calibration: a) Procedures for the generation, b) report on their validation

Final: 2013-07-30

Hanspeter Andres, Jürg Schlatter, Felix Lüönd (METAS)[1]

Athanasios Mamakos, Francesco Riccobono (JRC)[2]

Andreas Nowak, Anke Jordan-Gerkens (PTB)[3]

Thomas Tuch[4]

[1] Federal Institute of Metrology METAS, Switzerland
[2] Joint Research Centre (JRC), EC
[3] Physikalisch Technische Bundesanstalt (PTB), Germany
[4] Leibniz Institute for Tropospheric Research (TROPOS), Germany

CONTENT

1 SCOPE

Concerns related to the adverse health effects of automotive exhaust aerosols have driven the regulatory authorities worldwide to limit the particulate emissions of diesel vehicles. The particulate emission performance at a certification stage is traditionally monitored gravimetrically, by means of collecting samples from a Constant Volume Sampler (CVS). Recognizing that the gravimetric procedure would not be sensitive enough to discriminate between the very efficient wall flow Diesel Particulate Filters (DPFs) and flow through particulate filters, a particle number limit was introduced. It became effective at the Euro 5b stage (9/2011 – [1] [2]).

Introducing particle number measurements required new procedures for instrument validation and calibration. These procedures are based on the measurement of particles with defined mobility diameters between 23 nm and 100 nm [3]. The configuration of the measuring instrument is defined in detail and consists of a pre-conditioning unit and a measuring unit (Figure 1). The major component of the sample pre-conditioning system is a Volatile Particle Remover (VPR), which is used to define the characteristics of the particles to be measured. This basically involves the removal of volatile substances from the aerosol, as solid particles are the most relevant regarding health effects. The VPR provides heated dilution, thermal conditioning of the sample aerosol, a second dilution and cooling of the sample prior to entry into the measuring unit. The measuring unit consists of a particle number counter (PNC).

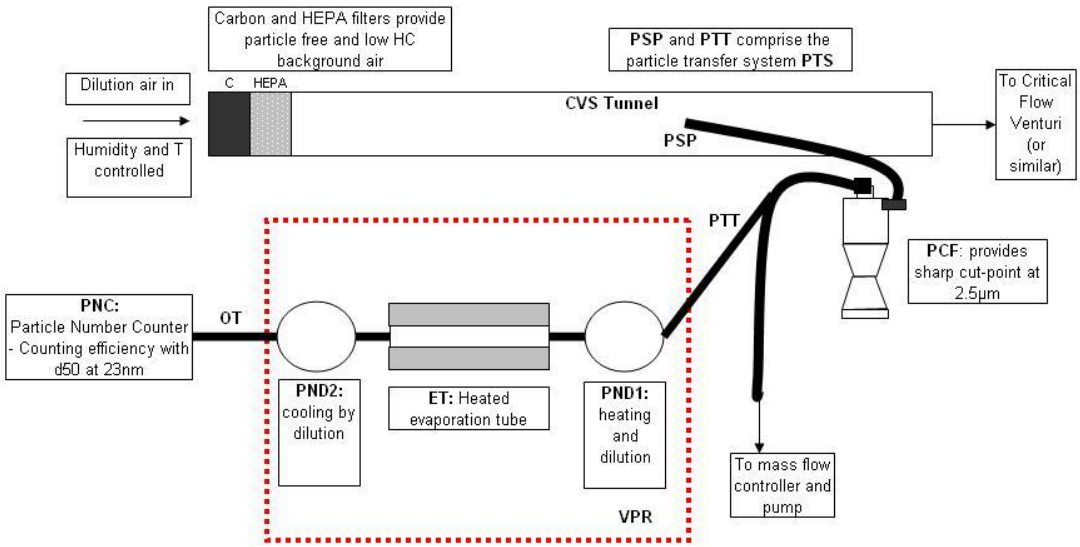

Figure 1: Schematic of recommended particle sampling system for exhaust particle measurements from a CVS-tunnel according to ECE Regulation 83 clause 1.4.4

The aim of the EMRP ENV02 "PartEmission" Work package 1 "*Automotive combustion particle metrics"* is to standardize calibration procedures for such measuring systems. The EMRP is jointly funded by the EMRP participating countries within EURAMET and the European Union.

Within the project the deliverable 1.1.2 deals with the generation of a test aerosol for the calibration of the VPR and the deliverable 1.1.3 deals with the generation of a test aerosol for the calibration of the PNC. This report summarizes the actions of the project partners preparing a test aerosol for the calibration of the VPR. The results fulfill the deliverable 1.1.2 from ENV02 “PartEmission”.

2 DESCRIPTION OF WORK IN ENV02

The project for ENV02 contract describes the work for the deliverable 1.1.2 in section C.1.a (see Table 1).

Table 1 Extract from the project contract ENV02

• Generation of aerosols to calibrate the number concentration in CPCs according to ECE regulations. These aerosols contain nanoparticles with unimodal size distributions, one single electric charge per particle, mobility diameters of 50 nm and 100 nm, and they are resistant to temperatures up to 300 °C. Various particle materials will be assessed: Oil based particles (MIKES, EJPD), combustion particles (EJPD, JRC-IE, PTB-3.2), salt particles (JRC-IE, PTB-3.2). The task delivers procedures on aerosol generation and adequate probes for subsequent assessment of the aerosols. (Deliverable: 1.1.2)
• Evaluation of the thermal stability of the 50 nm and 100 nm aerosols by comparing the size distribution and morphology without and with the thermal treatment in the VPR. The task delivers a report on the aerosol stability (EJPD, JRC-IE, MIKES). (Deliverable: 1.1.2)

After first discussions about the project steps MIKES proposed to bring in their know-how with SCAR (Single Charged Aerosol Reference) for deliverable 1.2.2 instead of deliverable 1.1.2. SCAR is an oil droplet generator with single charges on each particle. SCAR is a result from project iMERA-Plus project T3.J1.1. This proposal is appreciated by the JRP-Partners. Therefore three institutes instead of four work on this deliverable.

During the planning process the size range defined in the project description had to be expanded to the range defined in the ECE Regulation 83 by adding the particle size 30 nm.

3 VOLATILE PARTICLE REMOVER VPR

The requirements, the calibration and the validation of the VPR are defined in Regulation No. 83 in various sections as general requirements and recommended practice for VPR [1]. The next section summarizes the recommended system and the requirements. In the following sections the requirements for the temperature resistant aerosol are derived and a test procedure for the “thermal stability” of the aerosol is defined.

3.1 VPR Requirements and Recommended System

The requirements for the Volatile Particle Remover VPR in the sample preconditioning unit are defined in five clauses of ECE Recommendation R83 (Table 2). The major issues of these clauses are the heating of the aerosol up to 400 °C and the aerosol dilution.

Table 2 VPR requirements defined in ECE Recommendation No. 83, Revision 4, Annex 4a – Appendix 5

1.3.3.	The sample preconditioning unit shall:
1.3.3.1.	Be capable of diluting the sample in one or more stages to achieve a particle number concentration below the upper threshold of the single particle count mode of the PNC and a gas temperature below 35 °C at the inlet to the PNC;
1.3.3.2.	Include an initial heated dilution stage which outputs a sample at a temperature of ≥ 150 °C and ≤ 400 °C and dilutes by a factor of at least 10;
1.3.3.3.	Control heated stages to constant nominal operating temperatures, within the range specified in paragraph 1.3.3.2., to a tolerance of ±10 °C. Provide an indication of whether or not heated stages are at their correct operating temperatures.
1.3.3.4.	Achieve a particle concentration reduction factor ($f_r(d_i)$), as defined in paragraph 2.2.2., for particles of 30 nm and 50 nm electrical mobility diameters, that is no more than 30 per cent and 20 per cent respectively higher, and no more than 5 per cent lower than that for particles of 100 nm electrical mobility diameter for the VPR as a whole;
1.3.3.5.	Also achieve > 99.0 per cent vaporisation of 30 nm tetracontane ($CH_3(CH_2)_{38}CH_3$) particles, with an inlet concentration of ≥ 10,000 cm^{-3}, by means of heating and reduction of partial pressures of the tetracontane.

The deliverable 1.1.2 of the EMRP project deals with the generation of a test aerosol for the calibration of the VPR in the regarded particle size range. This aerosol shall be thermally stable, i.e. it shall not be altered in the VPR at 400 °C. However, testing the performance of the VPR in vaporizing the volatile fraction with tetracontane (see clause 1.3.3.5) is not subject of this project.

In the clauses about the recommended system (from clause 1.4.4) the realization of the VPR is described in a more concrete manner (see Figure 1). The recommended VPR comprises one particle number diluter (PND1), an evaporation tube (ET) and a second diluter (PND2) in series. This dilution function is to reduce the number concentration of the sample entering the particle concentration measurement unit to less than the upper threshold of the single particle count mode of the PNC and to suppress nucleation within the sample. The influence of the particle diameter on the particle concentration reduction factor (f_r) shall not exceed defined values.

The requirements shall be achieved with a dilution factor for the first dilution between 10 and 200, and the second dilution between 10 and 30.

3.2 Calibration of the VPR System

Calibration shall be undertaken by measuring the particle concentration reduction factor (f_r) at full range of applied dilution settings of solid particles with an electrical mobility diameter of 30, 50 and 100 nm. The number concentration range shall fit to the dilution range. Using above values of dilution ratios a concentration range (5×10^3 … 2×10^5) cm^{-3} is reasonable.

There are a number of aerosol generation techniques that are capable of producing solid particles in the size range between 30 and 100 nm diameter including condensation generators, combustion aerosol generators, and nebulization. Within the deliverable 1.1.2 various techniques shall be evaluated and described.

4 ASSESSMENT OF THE CALIBRATION AEROSOL

The calibration aerosol must be stable at VPR operating conditions, i.e. it should be physically and chemically stable and its aerodynamic behavior should not change at the evaporation tube operating temperatures. According to the drafted calibration procedures [3] the generation methods for the VPR calibration shall meet the following criteria:

- ✓ Capable of producing a stable aerosol at a minimum concentration of 5,000 cm^{-3} and below the single particle count mode limit of the particle number counter.
- ✓ Monodispersity: GSD ≤ 1.2.
- ✓ Relative humidity <50 % rH.
- ✓ The aerosol generation technique and aerosol material must produce a solid aerosol that is free from volatile particles (or a minimal fraction of volatiles).

The aerosols evaluated in this project are analyzed and documented in the subsequent sections according to Table 3.

Table 3 Documentation scheme of aerosols for VPR calibration

Characteristics	**Test method**	**Target results**
Particle Sizes	SMPS measurement	(30±3) nm, (50±5) nm, (100±10) nm Reproducibility: < 10 %
Concentration range	CPC or SMPS measurement	(5×10^3 … 2×10^5) cm^{-3}
GSD	SMPS measurement	< 1.2
Drift of size and concentration with time	CPC or SMPS measurement	Drift for size and concentration: < 10 %/h during 60 minutes
Humidity	Humidity measurement downstream a HEPA filter (if applicable)	< 50 %rH
Multiple charges	Tandem DMA measurement	Knowledge of charge distributions
Thermal size stability*	SMPS measurement*	Size shift < 5 %
Thermal number concentration stability*	SMPS measurement*	Concentration shift < 10 %, unless dilution or documented losses
Structural integrity*	Structure analysis of deposited particles with imaging methods*	no significant changes
Chemical composition*	Theoretical or analytical evaluation	no significant changes

* Comparison of characteristics upstream and downstream thermal treatment at 400 °C

5 GRAPHITE AEROSOL (JRC)

A PALAS DNP 3000 graphite spark generator was assessed at JRC. The particular unit was also employed as the reference instrumentation in a dedicated Inter-Laboratory Correlation Exercise (ILCE) organized by JRC aiming at the assessment of the comparability of the VPR calibration procedures established at different laboratories [4]. The thermal stability of the generated graphite particles was thoroughly investigated at eleven laboratories including JRC. The main limitation of these investigations was the relatively low temperature of the VPR system employed, which was set at 300°C. Accordingly, JRC conducted some additional dedicated investigations with an alternative VPR system operating at 350°C and 400°C. Here we focus on the results of the follow-up investigations conducted at JRC, which however are complemented by selected data from the ILCE.

5.1 Generation of the Graphite Aerosol

Particles in the PALAS DNP 3000 generator are produced in a spark discharge between two graphite electrodes. A stream of nitrogen flowing through the space between the electrodes transports the carbon evaporated in the spark. The carbon vapor then condenses to fine primary particles which subsequently coagulate to form bigger agglomerates. The peak size of the produced aerosol strongly depends on the concentration of the primary particles (which control the coagulation rate) which can be adjusted by means of varying the spark frequency. An internal dilution stage employing air as a diluent can suppress the rate of coagulation and thus provides an additional control of the produced size distribution. The only consumables in the PALAS DNP 3000 generator are the graphite electrodes that are supplied by PALAS.

The DNP 3000 instrument incorporates internal mass flow controllers to adjust the flows of nitrogen (3 to 20 lpm) and air (2 to 50 lpm) selected by the user. The control of the spark frequency is achieved through a high-voltage capacitor that is loaded through a multiplier by means of a direct current high voltage supply unit with adjustable output current. As soon as the breakdown voltage is achieved, the capacitor is discharged in a spark between the electrodes. The adjustable output current (0.5 to 7.3 mA) determines the loading time of the capacitor and accordingly the spark frequency. The distance of the electrodes (approximately 1.8 mm) is automatically adjusted to maintain the continuously monitored breakdown voltage (that increases with increasing electrode distance) constant. This close control of the breakdown voltage ensures a stable graphite production.

The produced particles are amorphous carbon aggregates with a primary particle diameter of 6.6±1.7 nm and a fractal dimension of 2.0±0.1 [5]. Furthermore, based on the operating principle of DNP 3000, the generated aerosol is volatile-free. Accordingly, there should not be a need for a stabilization of the produced aerosol. The operating settings chosen for the characterization of the DNP 3000 are summarized in Table 4. The generator was supplied with bottled nitrogen and HEPA-filtered, charcoal scrubbed and dehumidified (in a silica gel column) dilution air.

Table 4: Operating settings of the GAG employed for the PCRF measurements at 30, 50 and 100 nm at the different laboratories.

Parameter	Set point 1	Set Point 2
	30 nm	50 & 100 nm
Air flowrate [lpm]	6	3
Nitrogen flowrate [lpm]	3	3
Current [mA]	0.75	2

5.2 Characteristics of the Graphite Aerosol

The size distributions of the particles generated with the PALAS DNP 3000, were measured using a TSI 3936L10 Scanning Mobility Particle Sizer (SMPS), consisting of a TSI 3081 DMA, a TSI 3010 CPC and a 10 mCi ^{85}Kr neutralizer manufactured by Eckert and Ziegler GmbH. The SMPS operated at sheath and sample flowrates of 10 lpm and 1 lpm, respectively and at a scan time of 300 s. Owing to the high concentration of the generated aerosol, a TOPAS DDS 520 dilution bridge was employed to dilute the sample by 20:1 (set-point 1) to 60:1 (set-point 2). The residence time before this dilution step was also adjusted by means of using (conductive silicon) tubes of different lengths, or by adjusting the flowrate using an external pump sampling through a needle valve in parallel with the SMPS.

The measured size distributions are summarized in Figure 2. The results suggested a large coagulation potential owing to the high number concentrations of the produced aerosol (1.5×10^8 #/cm^3 with set point 2 and 6×10^7 #/cm^3 with set-point 1). Table 5 indicates the effect of residence time on the geometric mean diameter, geometric standard deviation and the total number concentration.

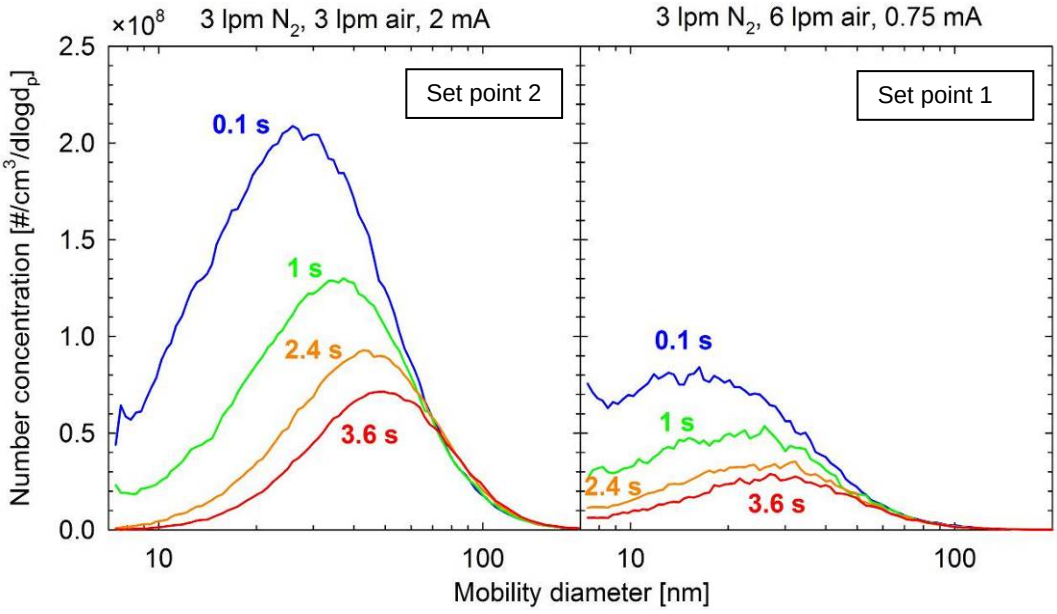

Figure 2: Number-weighted mobility size distributions measured at the two set-points of the DNP 3000 spark generator, for different residence times upstream of the dilution-bridge. The plotted distributions correspond to the average of at least two repetitions.

Table 5: Shift of the geometric mean diameter (d_g), the geometric standard deviation (s_g) and the total number concentration (N_{tot}), with increasing residence time upstream of the dilution stage. The ranges in parenthesis correspond to ± one standard deviation, derived from at least two repetitions.

Residence time [s]	0.1	1.0	2.4	3.6
Set point 1 – 3 lpm N_2, 6 lpm air, 0.75 mA				
d_g [nm]	18.3±0.1	20.9±0.4	23.9±0.1	25.6±0.3
s_g	1.79(±0.01)	1.80(±0.02)	1.80(±0.01)	1.79(±0.01)
N_{tot} [#/cm^3]	5.7(±0.1)×10^7	3.6(±0.1)×10^7	2.3(±0.1)×10^7	1.8(±0.1)×10^7
Set point 2 – 3 lpm N_2, 3 lpm air, 2.0 mA				
d_g [nm]	25.6(±0.3)	31.8(±0.4)	40.7(±0.23)	46.1(±0.8)
s_g	1.83(±0.01)	1.82(±0.01)	1.71(±0.01)	1.67(±0.01)
N_{tot} [#/cm^3]	1.5(±0.1)×10^8	8.3(±0.2)×10^7	5.2(±0.1)×10^7	3.9(±0.4)×10^7

The main parameter affecting the peak size of the generated aerosol is the current of the high voltage supply. The higher the current, the higher the peak diameter of the size distribution, but also the higher the frequency of discharges (10 to 350 Hz). The latter has a direct effect on the noise in the number concentrations of the generated aerosol. The 0.75 mA of set point 1 resulted in a rather low sparking frequency (~20 Hz) which led to more noisy distributions (as evident in Figure 2). However, in long term the generated aerosol was very stable. For example, size distribution measurements conducted 1 hour apart, yielded geometric mean diameters and total number concentrations that agreed within 1.5% and 3%, respectively, for both set points.

A suitable size distribution for calibration aerosol would result in limited classification of larger-, multiply-charged particles in Differential Mobility Analyzers (DMAs). The presence of multiply-charged particles is unavoidable and the best way to reduce their contribution is to ensure that the selected size lies as far away as possible (and above) from the mode of the distribution. The multiply charged fraction was quantified for the worst case condition[5] corresponding to a 3.6 s residence time (Table 5). For these investigations, a Tandem DMA setup was employed consisting of a Grimm 5.5-900 DMA connected in series with a TSI 3081 DMA. The two DMAs operated at a sheath flow rate of 3 lpm and a sample flowrate of 0.3 lpm. The first DMA was set at a fixed voltage corresponding to 30, 50 and 100 nm mobility diameter of singly charged particles, while the second operated in scanning mode (300 s). The Grimm DMA incorporated a 0.1 mCi ^{241}Am neutralizer (Grimm 5.522), while the TSI DMA was equipped with a 10 mCi ^{85}Kr neutralizer constructed by Eckert and Ziegler GmbH). The number concentrations of the TDMA classified particles were monitored with a TSI 3010 CPC. The DNP 3000 generator operated at set-point 1 for the 30 nm measurements and at set-point 2 for 50 and 100 nm.

The measured distributions are summarized in Figure 3. Three distinct peaks can be identified. The main one corresponds to the set diameter, while the larger one corresponds to doubly-charged particles classified in the first DMA that were subsequently neutralized at the entrance of the second DMA and then classified as singly-charged larger particles. A comparison of the concentrations of these two modes could serve as a rough estimate of the

[5] Typical residence times of graphite aerosols in particle concentration reduction factor measurements at JRC, were 1 to 2 s.

undesired fraction of multiply charged particles. This was found to be ~9% at 30 nm, ~13% at 50 nm and ~8% at 100 nm. Somehow lower multiply-charged fractions (down to 5%) were derived from TDMA measurements conducted at two other laboratories participating in the ILCE [4]. This was expected given the relatively large residence times of the produced poly-disperse aerosol in the tests at JRC, which led to significant coagulation and therefore shift of the distributions towards larger sizes.

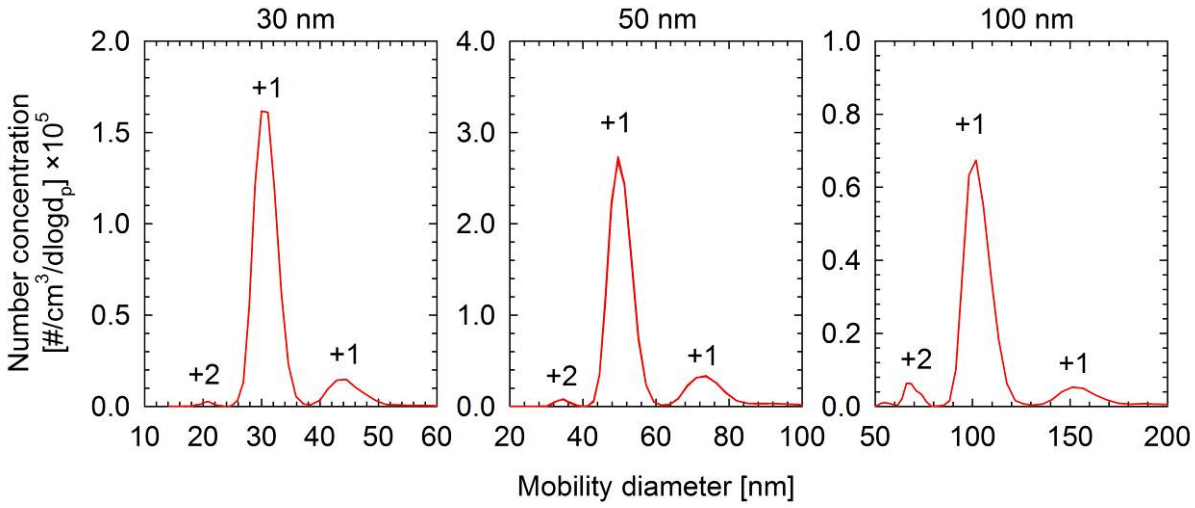

Figure 3: Number weighted mobility size distributions of DMA-classified 30, 50 and 100 nm graphite particles. The distributions have been corrected for diffusion losses and multiple-charged particles using the standard TSI inversion algorithm that assumes spherical particles.

The third mode at the smallest size corresponded to particles of the selected particle size that became doubly-charged after neutralization in the inlet of the second DMA. Given that the distributions were corrected for multiple charges using the standard TSI inversion algorithm that assumes spherical particles, the presence of this mode indicates that the aggregate graphite particles acquire more charges that spherical particles of the same mobility diameter. Indeed, this mode was not observed when performing similar tests with spherical emery oil droplets [4]. Again, a comparison of the concentrations of doubly and singly charged particles (from all three laboratories) suggested an excess fraction of 0.5-1% at 30 nm, 1.8-2.5% at 50 nm and 8.5-11% at 100 nm. This figures combined with the established charging probabilities for spherical particles [6], suggest that the probability that a graphite particle will acquire two charges in a neutralizer is ~50-70% higher compared to spherical particles of the same mobility. It should be stressed that these figures should be considered as rough estimates. An accurate determination of the charging probabilities should be rather based on comparison of TDMA signals with and without the neutralizer of the second DMA, as described in [7]. However, this was not possible at JRC given that the two DMA columns operated at opposite polarities [8]. Nevertheless, the results are in agreement with experimental data for the charging probabilities of Tungsten [9] and soot [10, 7] aggregates.

5.3 Temperature Resistance of the Graphite Aerosol

The thermal stability of the graphite particles was thoroughly investigated in the ILCE using a VPR system operating at 300°C [4]. Two laboratories measured the size distributions of DMA-classified particles, before and after passing the VPR system. Table 6 summarizes the geometric characteristics of the size distributions (d_g and s_g) upstream and downstream of the VPR, as well as the percentage differences. The geometric mean diameter was found to change by less than ±1%, while the geometric standard deviations agreed within ±0.5%. Note that the larger standard deviations (1.07-1.08 compared to 1.04-1.05) and the systematically higher diameters (3-5%) measured at lab 2 were to a certain extend attributed to the relatively low resolution of the SMPS employed (32 channels per decade).

Table 6: Comparison of the geometric mean diameter (d_g) and geometric standard deviation (s_g) of DMA-classified graphite particles of 30, 50 and 100 nm, upstream and downstream of a VPR operating at 300°C.

		30 nm		50 nm		100 nm	
		Lab 1	Lab 2	Lab 1	Lab 2	Lab 1	Lab 2
d_g [nm]	upstream	30.3	31.2	50.6	51.8	100.8	106.6
	downstream	30.1	31.4	50.3	52.0	99.7	106.3
	% change	-0.7%	+0.5%	-0.7%	+0.5%	-1.0%	-0.3%
s_g	upstream	1.042	1.077	1.040	1.079	1.051	1.085
	downstream	1.043	1.074	1.044	1.076	1.056	1.091
	% change	+0.1%	-0.3%	+0.3%	-0.3%	+0.5%	+0.5%

The ILCE also highlighted the sensitivity of particle concentration reduction factor (fr_{30}) measurements with thermally unstable 30 nm particles when a CPC with a 50% cut-off size (d_{50}) at 23 nm is employed. The reason for this sensitivity lies in the fact that a potential shrinkage of the 30 nm particles inside the VPR will result in reduced detection efficiency downstream of the VPR, and accordingly an underestimation of the downstream concentrations. Accordingly, three laboratories that performed this type of measurements with thermo-diluted CAST aerosol observed a 23 to 33% overestimation of the fr_{30} when employing the same CPC with a d_{50} at 23 nm [4]. However, such an effect could be determined in the graphite results obtained in nine laboratories [4].

All investigations in the ILCE were conducted at the nominal 300°C operating temperature of the reference VPR employed. Accordingly, JRC performed some dedicated investigations using an alternative VPR system (Nanomet from Matter Aerosol – [11]) operating at 350 and 400°C. The polydisperse aerosol produced by the DNP 3000 generator was size classified in the Grimm 5.5-900 DMA operating at sheath and sample flowrates of 3 lpm and 1 lpm, respectively. A TSI 3936L10 SMPS operating at sheath flowrate of 10 lpm, a sample flowrate of 1 lpm and a scan time of 300 s, was employed to measure the size distribution of the size classified particles at the exit of the DMA, or after passing the Nanomet. The investigations focused at 30 nm size which is the most sensitive size in *fr* measurements. The measured size distributions are summarized in Figure 4, while Table 7 compares the geometric mean diameters and the geometric standard deviations. In interpreting these results, it is important to consider that the dilution factor of the Nanomet

was approximately 300, and this led to relatively low concentrations (maximum CPC concentration was below 100 #/cm^3) downstream of the VPR. Despite that, the size distributions were broadly similar. The geometric mean diameter changed by less that 1% and the geometric standard deviation by less than 0.3%.

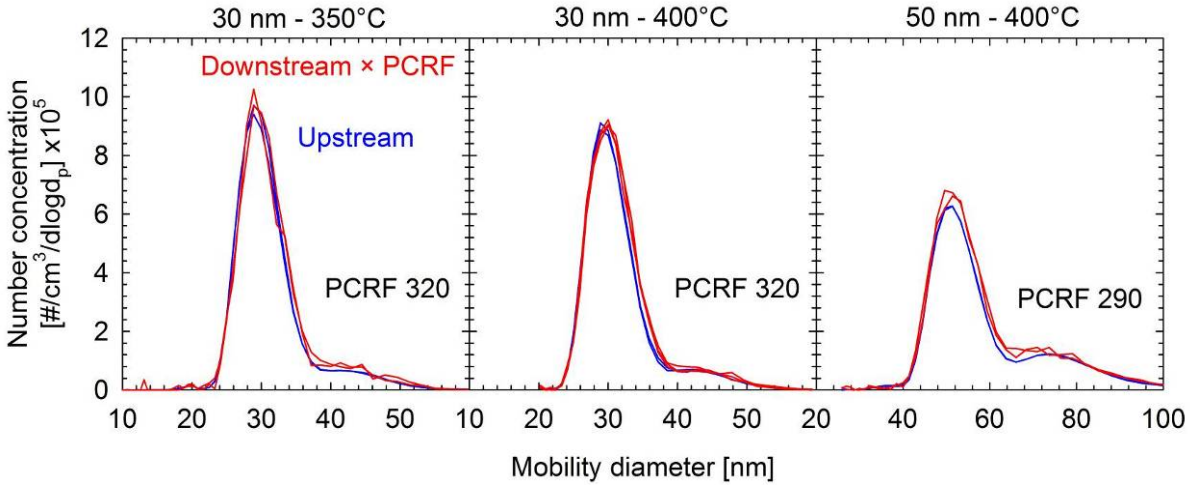

Figure 4: Measured size distributions of DMA classified graphite particles of 30 nm and 50 nm, upstream (blue lines) and downstream (red lines) of the Nanomet operating at 350°C and 400°C. The downstream distributions are corrected for the measured PCRF values (also shown in the graph).

In the context of particle concentration reduction factor measurements, what is of more importance is the effect of the distribution change on the fraction of particles detected by the CPC, owing to the finite detection efficiency of the instrument. The worst-case condition corresponds to a CPC designed around the PMP requirement of a d_{50} at 23 nm, in which case the 30 nm size resides at the steep part of the counting efficiency curve. Convolution of the TDMA distributions measured at JRC and the two laboratories from the ILCE (Figure 3) with experimentally determined detection efficiencies of a TSI 3790 CPC with graphite particles [12], suggested that the detected fraction would be affected by less than 1.5% (Figure 4).

Table 7: Comparison of the geometric mean diameter (d_g) and geometric standard deviation (s_g) of DMA-classified graphite particles of 30 and 50 nm, upstream and downstream of a VPR operating at 350 and 400°C.

		30 nm - 350°C	30 nm - 400°C	50 nm - 400°C
d_g [nm]	upstream	29.6	29.9	49.9
	downstream	29.9	30.2	50.1
	% change	+0.9%	+1.0%	+0.4%
s_g	upstream	1.110	1.111	1.109
	downstream	1.113	1.112	1.112
	% change	+0.3%	+0.1%	+0.3%

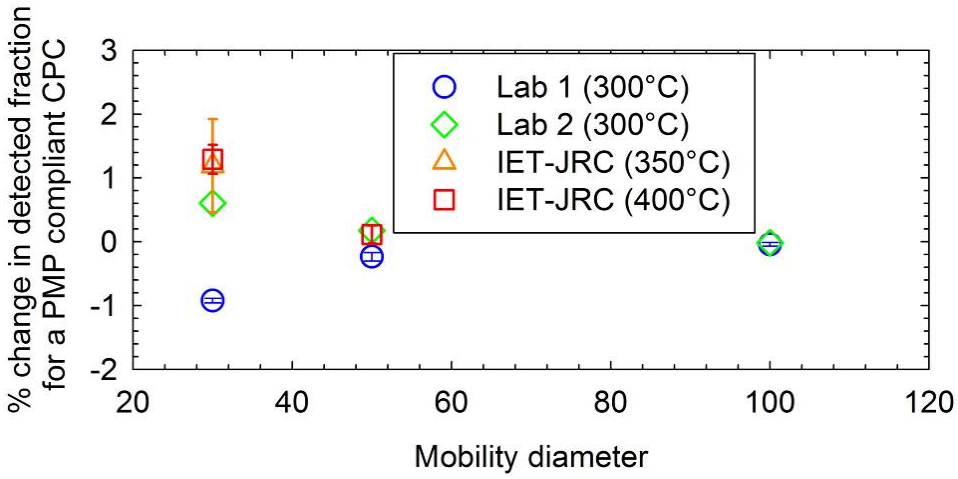

Figure 5: Simulated change of the fraction of particles detected with a TSI 3790 CPC, derived by convolution of the measured size distributions (Figure 4, [4]) and experimentally determined counting efficiencies for graphite particles [12].

6 COMBUSTION AEROSOL (METAS)

6.1 Generation of the Combustion Aerosol

A miniCAST generator was used to generate the combustion aerosol under investigation. In the combustion chamber, adjustable flows of propane, air and nitrogen are combined, and the flame is quenched by a nitrogen flow. The generator was combined with an active carbon based thermodenuder to eliminate volatile compounds from the primary aerosol. The thermodenuder (Topas TDD 590) consists of a heating section vaporizing volatile and semivolatile compounds of the aerosol and an adsorber section where the gaseous volatile fraction is adsorbed in active carbon and thus eliminated from the aerosol. The TDD 590 was operated at 400°C throughout the experiments, and additional measurements were conducted with the thermodenuder at room temperature in order to compare the thermal stability of the combustion aerosol with and without thermal treatment. The generation unit consisting of the miniCAST generator, a Topas DDS 560 diluter and the thermodenuder was tested regarding thermal stability of the aerosol downstream the thermodenuder. The corresponding experimental setup is displayed in Figure 6.

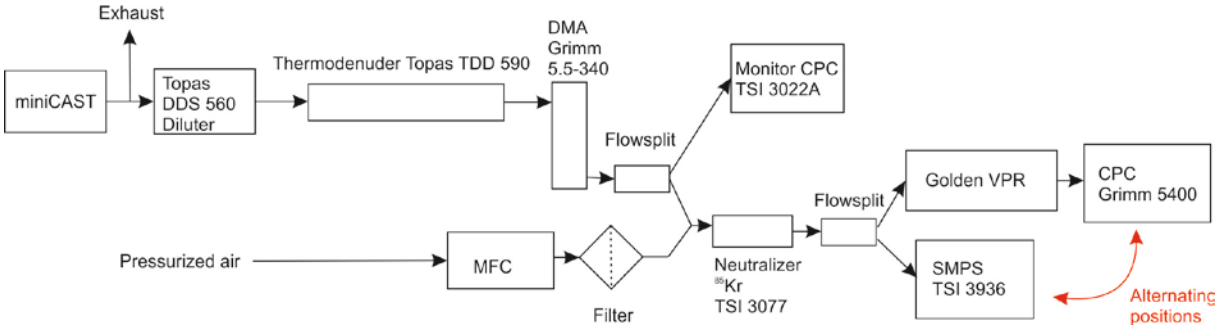

Figure 6: Experimental setup used to test thermal stability of the combustion aerosol generated by the miniCAST generator and thermally pre-treated by a thermodenuder

Downstream the generation unit, the aerosol was size selected by a Grimm DMA (5.5-340). Thermal stability was investigated by thermal dilution in the “Golden VPR” from JRC. The VPR consists of a primary heated dilution at 150°C, an evaporation section operated at 400°C and a second cooling dilution. We used an SMPS (TSI 3936 with 3085 or 3081 DMA) and a CPC (Grimm 5400) in alternating positions parallel to the VPR or downstream the VPR. SMPS measurements upstream and downstream the VPR revealed eventual changes in the size distribution due to evaporating volatile material, while the corresponding CPC measurements upstream and downstream the VPR provided the particle concentration reduction factor (PCRF) of the VPR. The injector diluters of the VPR were operated at a gauge pressure of 1 bar which resulted in an inlet flow rate between 2.7 lpm and 3.0 lpm at the inlet of the VPR, depending on the pressure upstream the VPR. This pressure depends on the dilution rate of the DDS 560 diluter, a lower dilution rate leading to a higher flow resistance of the diluter. During the experiments, it was necessary to adjust the dilution rate of the DDS 560 diluter either to ensure sufficient particle statistics downstream the VPR, or to avoid excessive particle concentrations upstream the VPR. Usually the Golden VPR is used at a gauge pressure of 2 bar instead of 1 bar. However, a reduced pressure leads to a smaller PCRF which allows for higher particle concentrations downstream the VPR. Furthermore, the vaporizing section can be expected to perform better at a reduced flow rate, which entails the tendency to a more rigorous test of thermal stability of the aerosol.

When the thermodenuder is operated at 400°C, its aerosol flow rate must not exceed 1 lpm to prevent smoldering in the active carbon. Smoldering has been observed as a massive production of particles inside the thermodenuder for aerosol flow rates above 1 lpm. We used a flow rate of 0.7 lpm, where smoldering has never been observed. Due to this relatively low sample flow as compared to the VPR inlet flow rate, a makeup air supply is required upstream of the VPR. We used the mass flow controller of the makeup air to tune the flow rate through thermodenuder and DMA. We used an old TSI 3077 neutralizer as a mixing volume to ensure thorough mixing of the aerosol with the makeup air.

A monitor CPC (TSI 3022A) was used downstream the DMA to normalize the number concentration measurements in order to eliminate eventual drift. With the monitor CPC operating at 0.3 lpm sample flow, a flow of 0.4 lpm size selected, thermally treated combustion aerosol is mixed with a makeup air flow between 2.3 lpm and 2.6 lpm, resulting in a dilution between roughly 1:6 and 1:8.

We used two different set points of the miniCAST generator as indicated in Table 8. Set point 1 corresponds to a rich combustion with a high ratio between fuel and air, set point 2 corresponds to a rather lean combustion.

Table 8: Gas flows in the combustion chamber of the miniCAST generator for two different set points used in the experiments

	Setpoint 1, rich combustion	Setpoint 2, lean combustion
Sizes	30, 50, 100 nm	100 nm
Gas flows:		
- Propane (C3H8)	30 ml/min	21 ml/min
- Air	0.5 l/min	0.62 l/min
- Nitrogen (N2)	0 ml/min	27 ml/min

6.2 Characteristics of the Combustion Aerosol

As the requirement of sufficient particle statistics downstream the VPR enforced high particle number concentrations upstream the DMA and hence a low dilution rate at the Topas diluter, coagulation significantly alters the size distribution between the exit of the miniCAST and the inlet of the DMA. Particle number concentration, geometric mean and standard deviation at the DMA inlet are summarized in Table 9 for the two used set points. Reported uncertainties were obtained from at least three repetitions with intermittent change of the set point of the miniCAST. We report values for a typical configuration with the Topas diluter operated at a dilution ratio of 1:8 (at a sample flow rate of 0.7 lpm), and for a configuration with the Topas diluter removed from the system. The latter configuration was required when 100 nm particles were selected at the DMA, for both set points: If 100 nm particles are selected from set point 1, the particle yield is low because the selection occurs in the tail of the size distribution. For set point 2, the overall particle concentrations are lower than for set point 1.

Table 9: Characteristics of the combustion aerosol at the inlet of the DMA for set point 1 and set point 2. Uncertainties represent the variability obtained from at least three repetitions.

	Setpoint 1, rich combustion	Setpoint 2, lean combustion
Sizes	30, 50, 100 nm	100 nm
Number conc. [cm-3]		
- Topas diluter 1:8	$(4.37 \pm 0.25)\cdot10^6$	$(1.84 \pm 0.17)\cdot10^6$
- No diluter	$(1.17 \pm 0.07)\cdot10^7$	$(8.1 \pm 0.8)\cdot10^6$
Geom. mean diameter [nm]		
- Topas diluter 1:8	37.3 ± 0.3	79 ± 2
- No diluter	62.1 ± 0.5	113 ± 3
Geom. std. dev.		
- Topas diluter 1:8	1.54 ± 0.01	1.69 ± 0.01
- No diluter	1.54 ± 0.01	1.61 ± 0.01

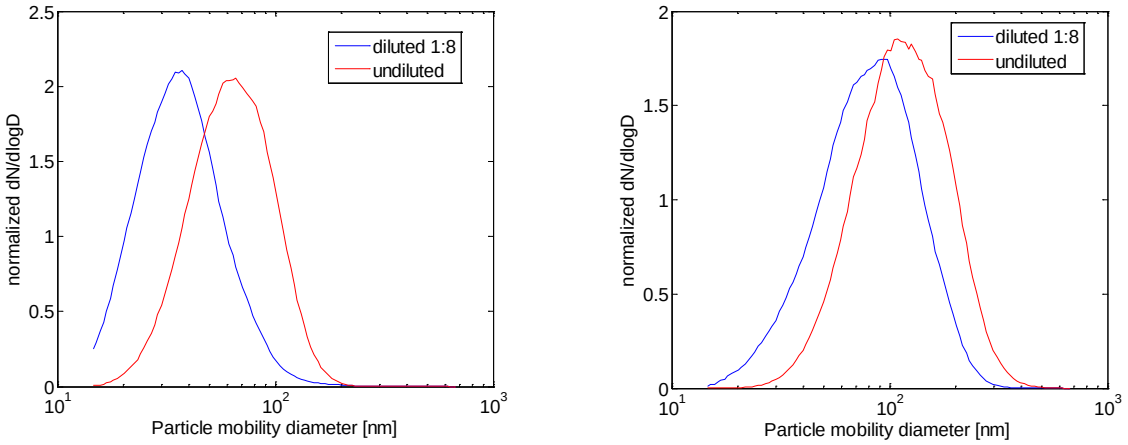

Figure 7: Size distributions at the DMA inlet for setpoint 1 (left panel) and setpoint 2 (right panel) for a diluted and an undiluted primary combustion aerosol.

It is obvious that the dilution of the primary aerosol has a major influence on the size distribution at the DMA inlet, in particular for the smaller sizes in set point 1 where the geometric mean diameter increases from 37.3 nm to 62.1 nm upon removing the Topas

diluter (see Figure 7). Increased coagulation also manifests in the number concentration, where the factor between the undiluted and the diluted concentration is significantly below the factor 8 expected from the setting of the Topas diluter.

Figure 8 displays SMPS size distributions of the size selected aerosol downstream the DMA for selected 30 nm, 50 nm and 100 nm particles. For 50 nm and 100 nm particles, a secondary peak is visible originating from doubly charged, larger particles. As mentioned previously, selection of 100 nm required an undiluted and therefore significantly coagulated aerosol. For set point 2, this resulted in a mode diameter of the input size distribution larger than the diameter selected at the DMA. This situation leads to a large fraction of multiply charged particles. In fact, the large fraction of multiple charges leads to a geometric standard deviation larger than 1.2 for 100 nm particles selected from set point 2 (see Table 12). For set point 1, the input size distribution peaks below the selected size, leading to significantly less multiply charged particles.

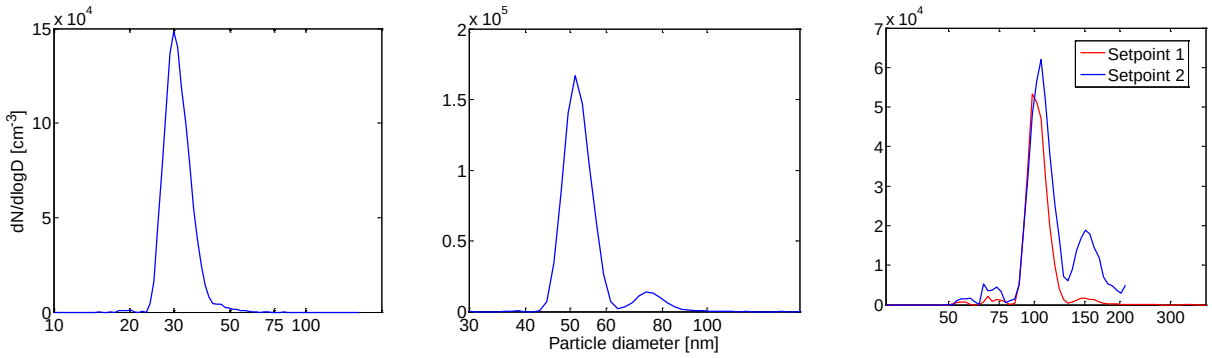

Figure 8: Measured size distributions of size selected combustion aerosol upstream the VPR for 30, 50, and 100 nm selected mobility diameter.

Using lognormal fits in order to estimate the number concentration in the individual charge levels leads to the fractions of multiply charged particles for the different selected particle sizes summarized in Table 10. Except from 100 nm particles selected from setpoint 2, multiply charged fractions are below 10%. The concentration range for thermally treated, size selected combustion particles upstream the VPR is also summarized in Table 10. For 30 nm particles, removing the diluter does not significantly increase the yield of 30 nm particles downstream the DMA, since the size distribution upstream the DMA shifts to larger sizes due to coagulation (see Figure 7). This results in a lower maximum concentration downstream the DMA compared to 100 nm particles, although the miniCAST generator produces significantly more 30 nm particles than 100 nm particles. A limiting factor for the obtainable concentration is the dilution by make-up air upstream the VPR (Figure 6). This might be circumvented by exchanging the positions of the VPR and the thermodenuder in the experimental setup. However, the thermodenuder has not been validated regarding its efficiency to remove volatile particles for a given flow rate.

Table 10: Concentration range and multiply charged particles fractions of size selected combustion particles upstream the VPR with thermal treatment (thermodenuder at 400°C) and without thermal treatment (thermodenuder at 30°C)

Particle size [nm]	Setpoint	Concentration range [cm^{-3}]	Thermodenuder Temp [°C]	Multiple charged fraction [%]
30	1	≤ 6‘000	30	n.a.
			400	2.6
50	1	≤ 10‘000	30	9.5
			400	6.7
100	1	≤ 20‘000	30	6.0
			400	8.0
	2	≤ 10‘000	30	30.0
			400	30.0

Long time stability of the particle diameter could be confirmed: After 1 h of continuous operation, a drift of the geometric mean diameter no larger than 3% towards smaller particle sizes was observed. Concerning particle number concentration, long time stability could be confirmed for setpoint 1: Small drifts both towards smaller and larger concentrations were observed with magnitudes below 4% over durations of at least 4000 s. For setpoint 2, a large negative drift of more than 30% over 3600 s was observed.

The humidity of a combustion aerosol can be considerable a priori, depending on the treatment after generation. As we could not use a diluter operating with dry, pressurized air, the relative humidity of the aerosol at the inlet of the thermodenuder was observed to be as high as 69%. While efficient in removing organic compounds from a gas, the thermodenuder cannot be expected to significantly reduce the relative humidity. Exposition to high relative humidity has been found to influence the size and structure of combustion aerosols by condensation of water vapor on sharp angle cavities of aggregate particles [13]. We therefore expect water vapor to condense to some unknown extent on the particles downstream the combustion chamber of the generator. However, due to the combustion particles being fresh and therefore hydrophobic in the present experiments, we do not expect a large amount of water to condense on the particles. Indeed, size shift of thermally treated aerosol in the VPR is small compared to the situation without thermal treatment, which suggests the possible amount of condensed water on the combustion aerosol to be small as compared to the amount of volatile organic material (see section 6.3).

6.3 Temperature resistance of the Combustion Aerosol

For the assessment of the temperature resistance of the combustion aerosol we concentrated on the eventual change of the geometric and mode diameter of the size selected aerosol within the VPR. The particle concentration reduction factor (PCRF) of the VPR might in principle provide complementary information on the thermal stability of an aerosol if it can be compared with the PCRF measured with a reference aerosol which is thermally stable. However, such a reference aerosol would have to exhibit equal particle morphology and material in order to attribute eventual differences in the PCRF between the reference aerosol and the aerosol under test to vaporization of volatile particles. As this is not realistic experimentally, we did not use PCRF as a measure for thermal stability. Measured sizes upstream and downstream the VPR are summarized in Table 11. Instead of the

geometric mean diameter, we used the mode diameter d_m of the singly charged particles to assess the change in diameter caused by the VPR. As the PCRF generally depends on particle size, a change of the fraction of multiply charged particles downstream the VPR might lead to a change in the geometric mean diameter of the size distribution even for thermally stable particles. A change in the mode diameter of singly charged particles can directly be attributed to thermal stability or instability. As the resolution of the mode diameter provided by the SMPS is limited by the bin size of the data inversion algorithm of the SMPS, we fitted lognormal distributions to the measured distributions of singly charged particles to obtain the corresponding mode diameter. In order to exclude the possibility of the observed size shifts to be due to condensed water evaporating from the particles in the VPR, we repeated the measurements with 100 nm particles selected from set point 1 with the DMA sheath air passing through a diffusion dryer. In this configuration, eventual condensed water evaporated from the particles in the DMA. This experiment is labeled “dry” in Table 11. Within the uncertainty, the size shift is equal with and without drying the DMA sheath air. This confirms the amount of condensed water on the combustion particles to be negligible. Table 12 summarizes the geometric standard deviations of the entire size distribution (i.e. including multiply charged particles) upstream and downstream the VPR.

Table 11: Mode diameter of singly charged size selected combustion particles upstream (up) and downstream (down) the VPR. Values for nominal 100 nm particles are reported for set point1 (s1) and set point 2 (s2). The label “dry” refers to a measurement with dried DMA sheath air.

Nominal size [nm]	Thermodenuder at 30°C			Thermodenuder at 400°C		
	d_m up	d_m down	change	d_m up	d_m down	change
30	n.a.	22.9 ± 0.3 nm	n.a.	30.7 ± 0.1 nm	30.3 ± 0.1 nm	-1.3 ± 0.5 %
50	51.8 ± 0.1 nm	39.8 ± 0.5 nm	-23 ± 1 %	51.3 ± 0.1 nm	50.6 ± 0.3 nm	-1.4 ± 0.7 %
100, s1	101.8 ± 0.1 nm	86.3 ± 0.9 nm	-15 ± 1 %	101.8 ± 0.1 nm	98.3 ± 0.2 nm	-3.4 ± 0.3 %
100, s1, dry	n.a.	n.a.	n.a.	101.0 ± 0.1 nm	97.5 ± 0.2 nm	-3.5 ± 0.2 %
100, s2	104.4 ± 0.3 nm	104.4 ± 0.8 nm	0 ± 0.8 %	104.3 ± 0.1 nm	103.1 ± 0.7 nm	-1.2 ± 0.7 %

Comparing mode diameters with a cold thermodenuder (30°C) and the thermodenuder operated at 400°C clearly show that the thermodenuder is necessary to thermally stabilize combustion particles from set point 1. Thermal treatment at 400°C results in an aerosol that changes by its mode diameter by no more than 1.4 % in the VPR for 30 and 50 nm particles. For 100 nm particles, the maximum change amounts to 3.5 % towards smaller particles for set point 1. Set point 2 provides a combustion aerosol which is thermally stable even without thermal treatment. However, the large fraction of multiply charged particles leads to a geometric standard deviation larger than 1.2 for set point 2. For set point 1, σ_g is well below 1.2 upstream the VPR, confirming sufficient monodispersity.

Table 12: Geometric standard deviation of the size distribution of combustion particles upstream (up) and downstream (down) the VPR. Values for nominal 100 nm particles are reported for set point1 (s1) and set point 2 (s2).

Nominal size [nm]	Thermodenuder at 30°C			Thermodenuder at 400°C		
	σ_g up	σ_g down	change	σ_g up	σ_g down	change
30	n.a.	1.24 ± 0.03	n.a.	1.09 ± 0.01	1.18 ± 0.04	+8 ± 4 %
50	1.14 ± 0.01	1.26 ± 0.03	+11 ± 3 %	1.13 ± 0.01	1.15 ± 0.01	+2 ± 2 %
100, s1	1.15 ± 0.03	1.23 ± 0.02	+7 ± 4 %	1.14 ± 0.04	1.14 ± 0.01	0 ± 4 %
100, s1, dry	n.a.	n.a.	n.a.	1.12 ± 0.01	1.13 ± 0.01	+1 ± 2 %
100, s2	1.22 ± 0.01	1.24 ± 0.01	+2 ± 2 %	1.23 ± 0.01	1.21 ± 0.02	-2 ± 2 %

For set point 1, Figure 9 shows lognormal fits of the measured size distributions upstream and downstream the VPR, the latter multiplied with the PCRF obtained from the CPC measurements.

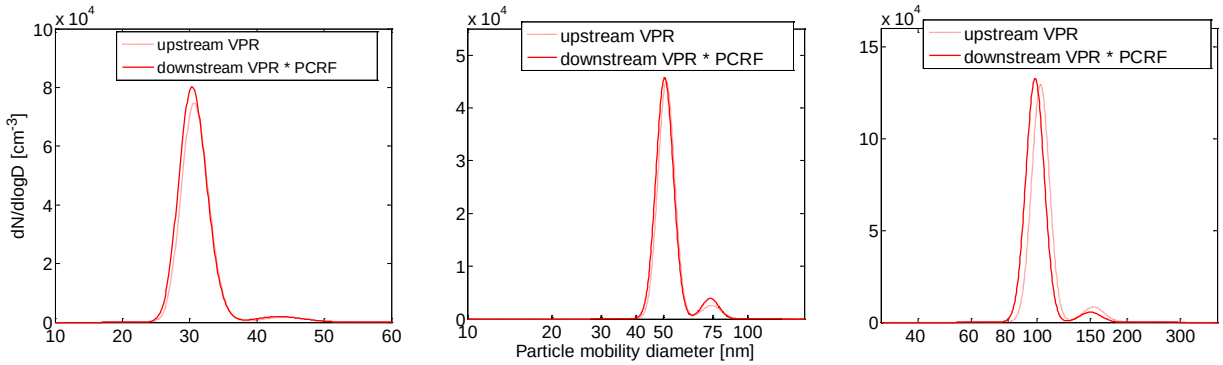

Figure 9: Lognormal fits of the size distributions measured upstream and downstream the VPR for nominal 30 nm (left panel), 50 nm (middle panel), and 100 nm (right panel) particles obtained from set point 1.

In summary, thermally treated combustion particles obtained from the rich combustion defined by set point 1 provide sufficient thermal stability and monodispersity for 30 nm, 50 nm and 100 nm particles, if the requirement concerning thermal stability is a change no larger than 5% in size upon exposition to 400°C, as formulated in Table 3. Also, we obtained a good reproducibility and long-time stability of the aerosol. The lean combustion defined by set point 2 allows for an improvement in thermal stability of 100 nm particles. However, due to a larger fraction of multiply charged particles, a geometric standard deviation below 1.2 cannot be achieved. Also, set point 2 does not meet requirements concerning long time stability of the particle number concentration.

7 SILVER AEROSOL (PTB)

7.1 Generation of the Silver Aerosol

For the deliverable 1.1.2, PTB worked together with the REG-partner (TROPOS; Thomas Tuch). For that reason the laboratory infrastructure at TROPOS was used for the generation of silver particles. For the description of the setup it will be split into two parts, part 1 is for the generation and dilution of silver particles (see figure 10) and part 2 consists of the measuring and sintering units (see figure 11).

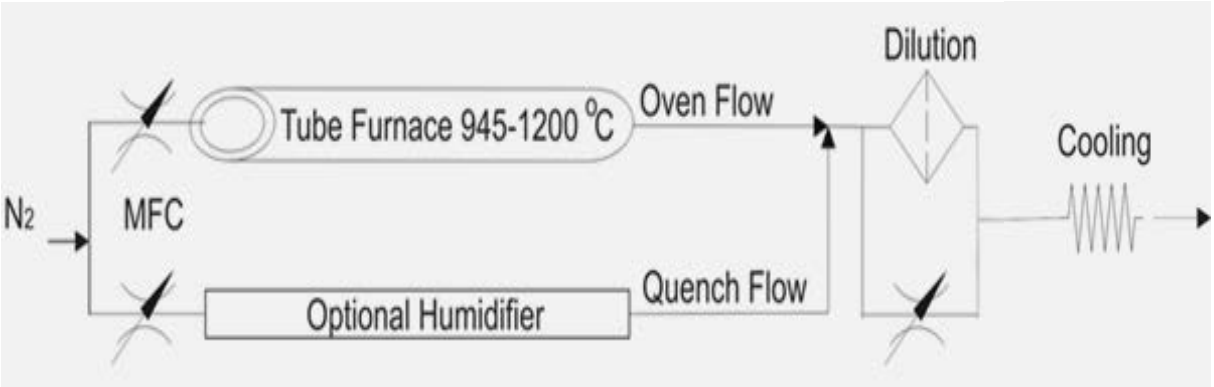

Figure 10: Schematic view of the generation and dilution part at TROPOS

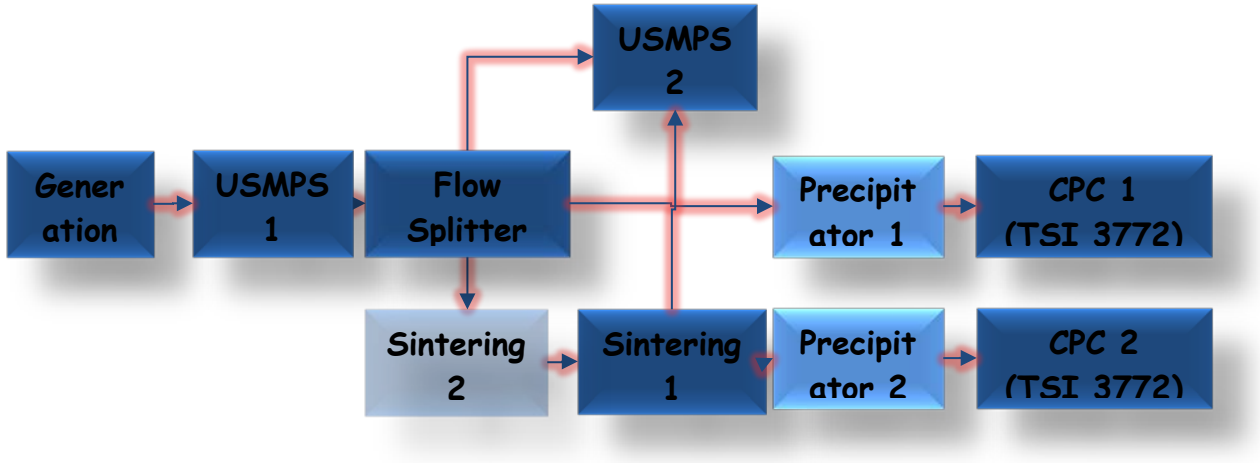

Figure 11: Schematic view of the measuring and sintering units at TROPOS

For the generation of silver particles a tube furnace with three temperature controlled heating zones (Linn model FRH-3-70/750/1250, Linn High Therm GmbH, Eschenfelden, Germany) was used. The sample material for evaporation is located in a boat in the center of a ceramic tube with in inner diameter of 19 mm. After the ceramic tube the oven flow and quench flow are mixed directly. A dilution part consisting of a filter and a manual bypass valve allows the adjustment of the particle number concentration. Behind the dilution a spiral is used to cool down the silver particles to room temperature.

After the cooling the silver particles enter the measuring and sintering unit (see figure 11). Before feeding the silver particles into the USMPS1 they have to be neutralized by a 370 MBq Kr85 neutralizer. A TROPOS made Hauke short DMA at an aerosol flow of 3 l/min and a sheath air flow of 20 l/min is used to selected monodisperse particle sizes. A second USMPS2 measured the monodisperse size distribution to check the stability of the particle generation with/without sintering. The USMPS2 was operated with an aerosol flow of 1 l/min and a sheath air flow of 10 l/min. Two particle precipitators were installed for two different lines to measure silver particles with and without thermal treatment by a sintering furnace at 400 °C. At the end of each line were implemented two identical CPC of the same company (TSI 3772) to estimate the total number concentration of deposited silver particles on TEM grids. For some studies a second furnace was installed to check the stability of thermal treated silver particles after passing by the first sintering furnace.

7.2 Characteristics of the Silver Aerosol

The characteristic of the setup is given by typical polydisperse size distributions of the generated silver particles and is shown in figure 12. Note the effect of flow rate settings at 1100 °C. At 1.5 l/min for both flows the oven size distribution is shifted to smaller particles at lower concentrations compared to an oven flow of 2.0 l/min and quench flow 5.0 l/min.

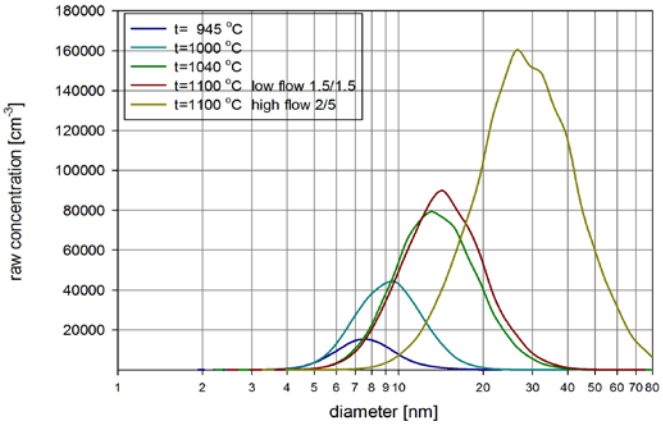

Figure 12: Schematic view of the measuring and sintering units at TROPOS

During the measurements PMP conform sizes classes like 15, 23, 41 and 50 nm were selected monodispersly by USMPS1. For the 100 nm silver particles the silver furnace does not work, because the maximum temperature is limited to 1200 °C. We tried to use silver particle in liquid from TedPella, but we could not find any particle in the particle number size spectra of USMPS 1. We attributed this to too less particles in the liquid.

7.3 Temperature Resistance of the Silver Aerosol

For the temperature resistance of silver particles several runs for different PMP size classes were performed. A sintering furnace was installed to check the stability of the mean diameter for the monodisperse particle number size distribution. We could observe clearly a shift in diameter after passing the sintering furnace; the larger the particles were the greater the shift in diameter was measured. Figure 13 exemplarily depicts the two sizes classes 15 and 23 nm, respectively.

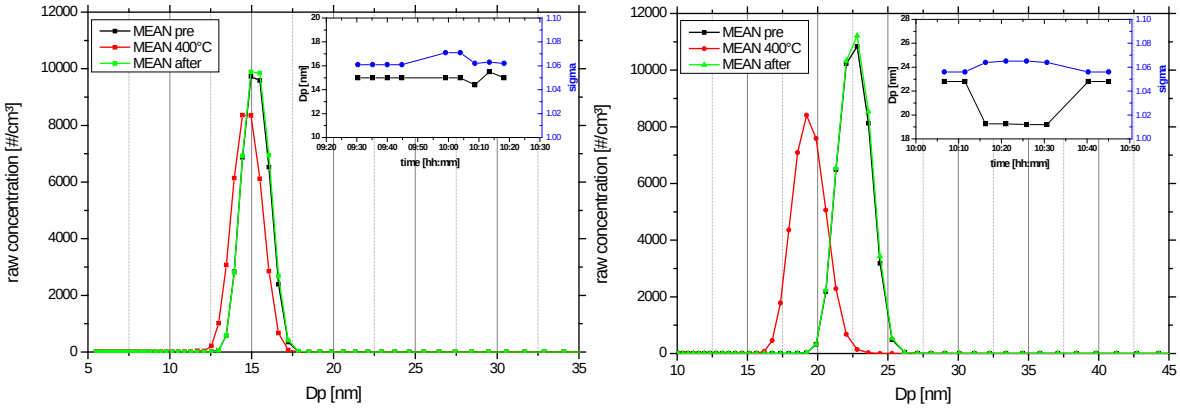

Figure 13: Monodispere distribution measured with USMPS2 and Gaussian fit parameter of distribution with diameter (dp) and width of mode (sigma) at left hand side for 15 nm and at right hand side for 23 nm respectively

After analyzing TEM grids by TESM showed similar results, see figure 14. We could explain the shift in diameter observed by measurements with UDMA, it's clearly a change in the morphology of silver particles.

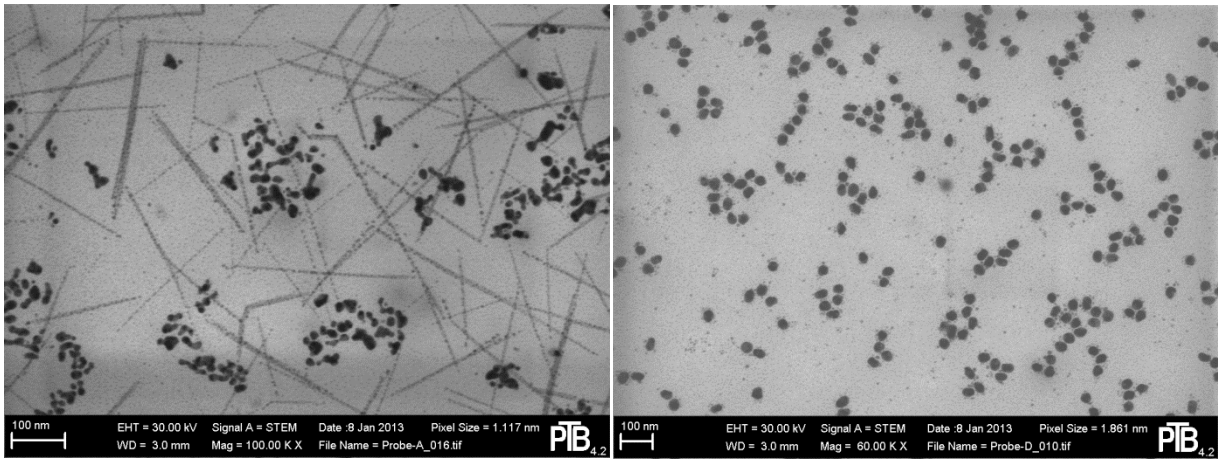

Figure 14: TESM pictures of non-sintered (left hand side) and sintered silver particles (right hand side) at 50 nm

Afterwards a second sintering furnace was implemented downstream the first sintering furnace into the setup. The results show a stable particle number size distribution before and after the second sintering furnace. Thus it can be assumed that the silver particle morphology does not change during the second sintering furnace.

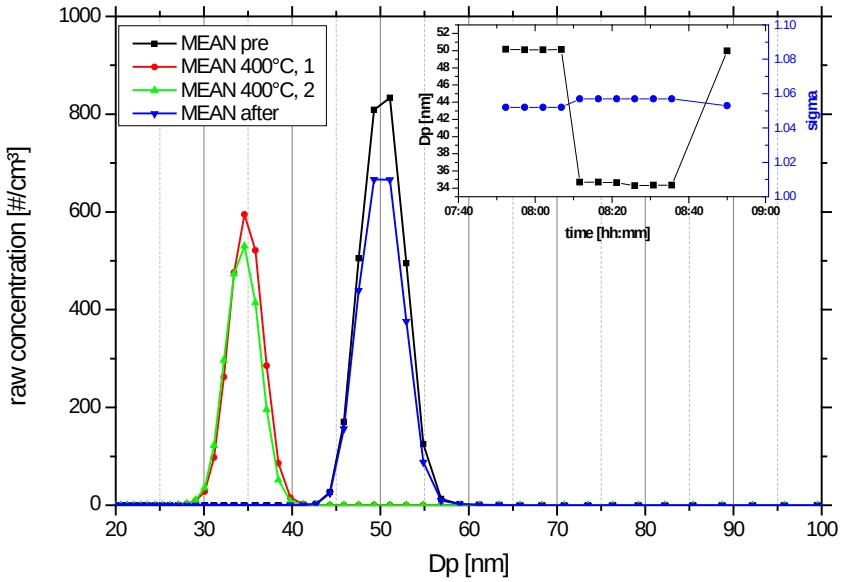

Figure 15: Monodispere distribution measured with SUDMPS2 and Gaussian fit parameter of distribution with mode diameter (dp) and width of mode (sigma) for a double sintering process

In summary, thermally treated silver particles obtained from nucleation furnace provide sufficient thermal stability and monodispersity for 15 nm, 23 nm, 41 nm and 50 nm particles only after implementation of a sintering furnace as well as after monodisperse selection of a UDMA. Otherwise, non spherical silver particle were observed (see table 13).

Table 13: Mode diameter of selected combustion particles before, during and after (down) the sintering process

Nominal size [nm]	before at 23°C		during at 400°C		After at 23°C	
	Dp mode	Sigma	Dp mode	Sigma	Dp mode	Sigma
15	15	1.06	15	1.07	15.2	1.06
23	22.8	1.06	19.2	1.06	22.8	1.06
41	40.8	1.05	29.93	1.06	40.8	1.05
50	50.1	1.05	34.6	1.06	50	1.05

8 SUMMARY AND CONCLUSIONS

The coordinated actions of the partners involved in this part of the JRP ENV02 project have led to the following achievements which accomplish the tasks for deliverable D1.1.2.

- The combustion aerosol was generated using a miniCAST (combustion aerosol standard). The miniCAST can be operated either in a fuel-lean or fuel-rich combustion mode; the latter presumably producing less thermally stable particles due to the increased VOC (volatile organic compounds) fraction. By using a PALAS thermodenuder thermal stability up to 400 °C was demonstrated by use of the “golden” VPR from JRC-IE for the more critical fuel-rich combustion mode. Thermal stability is good for thermally treated 30 nm and 50 nm particles, and still sufficient for 100 nm. The maximal particle number concentration is in the order of 10^4 cm^{-3}.
- Silver aerosols were generated using a nucleation oven at temperatures up to 1100 °C with and without a sintering oven operated at 400 °C downstream. During sintering the nucleated silver particles shrink by 1 nm to 17 nm in the size range 15 nm to 50 nm, respectively. By using a setup with two sintering ovens thermal stability of the sintered silver particles was demonstrated. The achievable maximum silver particle size is limited to 50 nm.
- An aerosol of graphite particles was generated using the PALAS spark generator DNP300. Particles in this generator are produced in a spark discharge between two graphite electrodes. By varying the spark frequency and the diluting air flow particle sizes in the range between 20 nm and 100 nm are generated. Particle number concentrations up to 10^7 cm^{-3} are achievable. The thermal stability of the particles was verified up to 400 °C. Observed particle diameter changes are below 1 %.

For all three calibration aerosols thermal stability up to 400 °C was demonstrated. The calibration aerosol with silver particles is limited by the achievable maximum particle size. The combustion and graphite aerosol prove suitable for the entire size range.

9 REFERENCES

[1] Regulation No. 83: Uniform provisions concerning the approval of vehicles with regard to the emission of pollutants according to engine fuel requirements
http://www.unece.org/fileadmin/DAM/trans/main/wp29/wp29regs/r083r4e.pdf

[2] Commission Regulation (EC) No 692/2008 of 18 July 2008 implementing and amending Regulation (EC) No 715/2007 of the European Parliament and of the Council on type-approval of motor vehicles with respect to emissions from light passenger and commercial vehicles (Euro 5 and Euro 6) and on access to vehicle repair and maintenance information. http://eur-lex.europa.eu/LexUriServ/LexUriServ.do?uri=OJ:L:2008:199:0001:0136:EN:PDF

[3] AEA Energy & Environment; Volatile Particle Remover - Calibration and Validation Procedures , ED47382004/VPR, Issue Number 5, December 2007 http://www.unece.org/fileadmin/DAM/trans/doc/2008/wp29grpe/PMP-VPR-CalibrationProcedure.pdf

[4] Mamakos A., Martini G. and Krasenbrink A. (2012a). Particle Measurement Programme. Volatile Particle Remover Calibration Round Robin. Final Report. JRC Scientific and Policy Report EUR XXXXX EN.

[5] Wentzel, M., Gorzawski, H., Naumann, K.-H., Saatho, H. and Weinbruch S. (2003). Transmission Electron Microscopical and Aerosol Dynamical Characterization of Soot Aerosols. Journal of Aerosol Science, 34:1347-1370.

[6] Wiedensohler A. (1988). An Approximation of the Bipolar Charge Distribution for Particles in the Submicron Size Range. Journal of Aerosol Science, 19: 387-389.

[7] Maricq, M.M. (2007). Bipolar Diffusion Charging of Soot Aggregates. Aerosol Science and Technology, 42:247-254.

[8] Mamakos, A., Giechaskiel, B. and Drossinos, I., Lesueur, D., Martini, G. and Krasenbrink, A. (2011a). Calibration and Modelling of PMP-Compliant Condensation Particle Counters. JRC Scientific and Technical Research Report, EUR 25145 EN. Available at: http://publications.jrc.ec.europa.eu/repository/handle/111111111/25454

[9] Rogak, S., N. and Flagan R., C. (1992). Bipolar Diffusion Charging of Spheres and Agglomerate Aerosol Particles. Journal of Aerosol Science, 23:693–703.

[10] Lall, A., A. and Friedlander, S. K. (2006). On-line Measurement of Ultrafine Aggregate Surface Area and Volume Distributions by Electrical Mobility Analysis: I. Theoretical Analysis. Journal of Aerosol Science, 37:260–271.

[11] Kasper M. (2004). The Number Concentration of non-Volatile Particles – Design Study for an Instrument According to the PMP Recommendations. SAE Technical Paper 2004-01-0960.

[12] Mamakos A., Giechaskiel B., Drossinos Y., Lesueur D., Martini G. and Krasenbrink A. (2011). Calibration and Modeling of PMP Compliant Condensation Particle Counters. JRC Scientific and Technical Report EUR 25145 EN.

[13] Weingartner E., Baltensperger U., and Burtscher H. (1995). Growth and Structural Change of Combustion Aerosols at High Relative Humidity. Environ. Sci. Technol. 29, p. 2982 – 2986.